Supplementary Appendix To:

Identification of novel pathogenic genes of childhood epileptic encephalopathies

Yi-Wu Shi[1*], Jian-Guo Zhang[2,3*], Na He[1*], Zi-Long Ye[1], Wen-Bin Li[1], Han-Kui Liu[2,3], Zhi-Gang Liu[4], Nan-Xiang Shen[1], Xiao-Chong Qu[1], Cui-Xia Fan[1], Jie Wang[1], Sheng Luo[1], Yu-Dan Lv[5], Li Gao[6], Jing Chen[7], Shao-Ping Huang[8], Xin-Guo Lu[9], Jing Yu[10], Jie Zhang[11], Xiu-Xia Wang[12], Qu-Wen Gao[13], Li Jiang[14], Yan-Hui Chen[15], Hui Qi[6], Jing-Da Qiao[1], Li-Zhi Chen[1], Yuan-Jin Zeng[1], Xiao-Xue Yang[16], Hong-Jun Yan[17], Cheng-Yan Li[18], Tao Zeng[19], Fu-Li Min[19], Bing Qin[20], Hai-Qing Xu[21], Lin Xu[22], Bing-Mei Li[1], Yong-Hong Yi[1], Zhi-Hong Zhuo[23], Qing-Hui Guo[24], Su-Li He[25], Hong-Wei Zhang[26,27], Li-Ping Guan[2,3], Wei-Yi Deng[1], Xiao-Fan Ren[9], Dong-Fang Zou[9], Wei-Yue Gu[28], Tao Su[1], Xiao-Rong Liu[1], Yi-Bo Qu[29], Xin-Ping Yang[16], Wei-Ping Liao[1#]

1 Department of Neurology, Institute of Neuroscience, Key Laboratory of Neurogenetics and Channelopathies of Guangdong Province and the Ministry of Education of China, The Second Affiliated Hospital, Guangzhou Medical University, Guangzhou, China, 510260

2 BGI Genomics, Shenzhen 518083, China

3 Clin Lab, BGI Genomics, Shijiazhuang 050011, China

4 Affiliated Foshan Maternity and Child Healthcare Hospital, Southern Medical University, Foshan, China

5 The First Hospital of Jilin University, Jilin, China

6 Department of Pediatrics, Henan Province People's Hospital, People's Hospital of Zhengzhou University, Zhengzhou, China

7 Department of Neurology, Children's Hospital of Nanjing Medical University, Nanjing, China

8 The Second Affiliated Hospital of Xi'an Jiaotong University, Xian, China

9 Shenzhen Children's Hospital, Shenzhen, China

10 Neurology Department, Children's Hospital of Xinjiang Uygur Autonomous Region, Urumchi, China

11 Hunan Provincial Children's Hospital, Changsha, China

12 The Second Hospital of Hebei Medical University, Shijiazhuang, China

13 Department of Neurology, Foresea Life Insurance Shaoguan Hospital, Shaoguan, China

14 Children's Hospital of Chongqing Medical University, Chongqing, China

15 Department of Pediatrics, Fujian Medical University Union Hospital, Fuzhou, China

16 Center for Genetics and Developmental Systems Biology, Nanfang Hospital, Southern Medical University, Guangzhou, China

17 Guangdong 999 Brain Hospital, Guangzhou, China

18 Affiliated Hospital of Guangdong Medical University, Zhanjiang, China

19 Guangzhou First People's Hospital, Guangzhou, China

20 The First Affiliated Hospital of Jinan University, Guangzhou, China

21 Xuzhou Center Hospital, Xuzhou, China

22 Qingdao Women and Children's Hospital, Qingdao, China

23 The First Affiliated Hospital of Zhengzhou University, Zhengzhou, China

24 The Second Hospital of Shandong University, Jinan, China

25 Shantou Chaonan Minsheng Hospital, Shantou, China

26 Children's Hospital Affiliated to Shandong University, Jinan, China

27 Jinan Children's Hospital, Jinan, China

28 Chigene (Beijing) Translational Medical Research Center Co., Beijing, China

29 Key Laboratory of CNS Regeneration (Ministry of Education), Guangdong-Hong Kong-Macau Institute of CNS Regeneration, Jinan University, Guangzhou, China

* These authors contributed equally to the manuscript.

Correspondence to Dr. Liao, Department of Neurology, Institute of Neuroscience, Key Laboratory of Neurogenetics and Channelopathies of Guangdong Province and the Ministry of Education of China, The Second Affiliated Hospital, Guangzhou Medical University, Guangzhou, China, E-mail wpliao@163.net; liao@gzneurosci.com.

Table of Contents

Supplementary Methods

Study patient enrollment

Among 235 cases, 194 were long-term follow-up patients in the Epilepsy Center of the Second Affiliated Hospital of Guangzhou Medical University. The other 41 patients were from 20 epilepsy centers in China, including the First Hospital of Jilin University, Affiliated Foshan Maternity and Child Healthcare Hospital, Guangdong 999 Brain Hospital, Henan Province People's Hospital, Shenzhen Children's Hospital, Hunan Provincial Children's Hospital, The Second Affiliated Hospital of Xi'an Jiaotong University, Foresea Life Insurance Shaoguan Hospital, Children's Hospital of Nanjing Medical University, People's Hospital of Xinjiang Uygur Autonomous Region, The Second Hospital of Hebei Medical University, Affiliated Hospital of Guangdong Medical University, Guangzhou First People's Hospital, The First Affiliated Hospital of Jinan University, Xuzhou Center Hospital, Qingdao Women and Children's Hospital, The First Affiliated Hospital of Zhengzhou University, The Second Hospital of Shandong University, Shantou Chaonan Minsheng Hospital, and Qilu Children's Hospital of Shandong University (Table S1). Detailed clinical information was collected, including sex, seizure onset age, seizure type and frequency, course of seizure, response to antiepileptic drugs, family history, and findings from general and neurological examinations. Brain MRI scans were performed to identify abnormalities in brain structure. Patients with acquired etiologies were excluded. Video EEG was examined, and the results were reviewed by two qualified electroencephalographers.

Epileptic seizures and Lennox-Gastaut syndrome (LGS) were diagnosed and classified in accordance with the Commission on Classification and Terminology of the International League Against Epilepsy criteria (1989, 2001, 2010, 2017, and 2022).

Whole-exome sequencing (WES)

Genomic DNA was extracted from the peripheral blood obtained from the patients and their parents (trios) using the QIARamp Blood Mini Kit (Qiagen, Hilden, Germany). Trio-based WES was performed on a HiSeq 2000 system (Illumina, San Diego, CA, USA) as previously reported[1,2]. The sequencing data were generated by massively parallel sequencing with > 100 times average depth and > 98% coverage of the capture regions, and the high-quality reads were mapped to the Genome Reference Consortium Human Genome build 37 (GRCh37) by Burrows-Wheeler alignment. Single-nucleotide variants and insert/deletion variants were called with the Genome Analysis Tool Kit.

Statistical analysis

For excess *de novo* variants, the *P*-value was calculated as [1-Poisson cumulative distribution function (χ-1, λ)], where χ is the observed *de novo* variant number for a specific gene, and λ is calculated as $2\times234\times1.2\times10^{-8}\times$effective transcript length of the gene on the autosome[3]. For excess biallelic variants, the *P*-value was calculated as [1-cumulative binomial probability [(n-1, N, R)], where n is the observed biallelic variant number for a specific gene, N is the number of trios (234 in this cohort), and R is the rate of variants in the gene by chance in the population[4]. The variants were filtered by

different MAF cutoffs based on the class of variants, i.e., biallelic loss-of-function (LOF), one LOF and one damaging missense, and biallelic damaging missense. Considering that all patients were Han Chinese, the cutoff was set according to the MAF in the ExAC-East Asian population. For the aggregated frequency of variants, the controls include a cohort of 296 healthy Chinese volunteers as in our previous report[2] and the control populations in gnomAD. It is currently unknown the frequencies of compound heterozygous variants in general populations. To analyze the significance of the compound heterozygous variants, we established a control cohort that included 1942 asymptomatic parents from trios, in whom the compound heterozygous variants were identified by detecting one of the paired variants in the child, given that one of the paired variants in a parent would transmit to the child.

Protein structure modeling

The tertiary structure of the protein encoded by the novel candidate genes was modeled using trRosetta (https://yanglab.nankai.edu.cn/trRosetta/) to predict the effect of missense variants on protein structure. Hydrogen bonding was analyzed and visualized using PyMOL 2.3 software (https://pymol.org/2/).

Fly stocks

Flies were fed standard cornmeal and maintained in an incubator at 25 ℃ and 60%-70% humidity on a 12:12-hr light/dark cycle as previously described[2]. The *Drosophila* homologs of the human *SBF1*, *CELSR2*, and *TENM1* genes are *Sbf* (CG6939),

Flamingo (CG11895), and *Ten-m* (CG5723), respectively. *UAS-Sbf-RNAi* (FBgn0025802), *UAS-Flamingo-RNAi* (FBgn0024836), and *UAS-Ten-m-RNAi* (FBgn0004449) were purchased from the Tsing Hua Fly Center (Tsinghua University, Beijing, China). The Gal4 driver lines *tub-Gal4* and *Canton-S* were gifts from Prof. Liu Jiyong (Guangzhou Medical University, Guangzhou, China). Virgin *tub-GAL4* females were mated with males of each RNA interference (RNAi) line to establish flies with specific gene knockdown. The RNAi efficiency of the three genes in flies was detected by reverse transcription quantitative PCR (RT-qPCR). *Canton-S* was used as the WT line in this study. Compared to WT flies, mRNA expression of the three genes in the knockdown flies was reduced by 47% (*Sbf*), 75% (*Flamingo*), and 79% (*Ten-m*) (Fig. S2). The primer sequences are listed in Table S2.

Seizure behavior test in flies

The *tub-Gal4* line was crossed with *Sbf-*, *Flamingo-*, and *Ten-m-RNAi* to establish globally corresponding gene knockdown flies (*tub-Gal4>Sbf-RNAi*, *tub-Gal4>Flamingo-RNAi*, and *tub-Gal4>Ten-m-RNAi*, respectively)[5]. The bang-sensitivity (BS) test was carried out on flies 3-5 days after eclosion, and seizure-like behavior was evaluated as described in previous studies[2,6]. Briefly, flies were anesthetized with CO_2 and transferred into a new clean food vial one day before testing. Three to six flies were placed in one vial and mechanically stimulated with a vortex mixer (VWR, Radnor, PA, USA) at maximum speed for 20 sec. The percentage and duration of BS paralysis in flies were recorded.

Electrophysiological assay on flies

Attached recording was performed in the knockdown and control flies using an established electrophysiological method[7]. Fly brains were dissected as previously described[8], transferred to a recording chamber with fly external solution, and immobilized with a C-sharp holder. The anterior side of the brain was positioned facing upward to enable observation of the soma of projection neurons (PNs) on the brain surface. The standard external solution contained 101 mM NaCl, 1 mM $CaCl_2$, 4 mM $MgCl_2$, 3 mM KCl, 5 mM glucose, 1.25 mM NaH_2PO_4, and 20.7 mM $NaHCO_3$ (pH 7.2, 250 mOsm). Attached recording was done by the Axon MultiClamp 700B amplifier with internal solution (contained 102 mM K-gluconate, 0.085 mM $CaCl_2$, 1.7 mM $MgCl_2$, 17 mM NaCl, 0.94 mM EGTA, and 8.5 mM HEPES (pH 7.2, 235 Osm)) filled glass pipettes (10-14 MΩ). Data were acquired with a Digidata 1440B digital–analog converter (Molecular Devices, San Jose, CA, USA) and pClamp v10.5 software (Molecular Devices, San Jose, CA, USA).

Generation of *sbf1* knockout zebrafish using CRISPR-Cas9

The AB strain zebrafish (provided by Dr. Yang Xinping of Southern Medical University) embryos and larvae were maintained on a 14:10-hr light/dark cycle and raised as previously described[9]. The larvae were allowed to develop at 28.5 ℃ and were staged by hours or days after fertilization under standard conditions. CRISPR-Cas9 genomic editing was used to generate *sbf1* knockout zebrafish as described previously[10].

SET binding factor 1 (encoded by *SBF1*) in humans and zebrafish is 70% identical. A germline mutation with a 4-nt (TGGA) deletion was introduced in exon 3 of the primary *sbf1* transcript (RefSeq: NM_001045158.1), resulting in a premature stop codon in exon 5 (Fig. S3A). The CRISPR target sequence (5'-AGTGGATGGCAGCTGGCTCC-3') and oligonucleotide were designed using ZiFit software[11]. The *sbf1*-targeting single-guide RNA (sgRNA) template plasmid was generated by annealing oligonucleotides and ligation of the double-stranded DNA in the plasmid PMD-18T (Takara, 6011) and then transcribed *in vitro* with T7 RNA polymerase (Thermo Fisher, # EP0111). A 1 nL mixture containing approximately 300 ng/μL Cas9 protein (New England Biolabs, Beverly, MA) and 15 ng/μL sgRNA was injected into one-cell stage embryos using a Picospritzer III pressure ejector. The mutant was verified by PCR-Sanger sequencing with dF1/dR1 primers.

The expression level of *sbf1* was detected in 5 days postfertilization (d.p.f) larvae by RT-qPCR using primers gF1/gR1 and dF2/dR2 and SYBR Premix Ex Taq (Takara, Japan) on an Mx3005P qPCR System (Agilent, USA). We confirmed that there was an absence of 88% of total *sbf1* mRNA in *sbf1*$^{-/-}$ and 41% of total *sbf1* mRNA in *sbf1*$^{+/-}$ zebrafish, proving the efficiency of the *sbf1* knockout (Fig. S3B). The primer sequences are listed in Table S2.

Morphological, survival, and behavioral analysis of *sbf1* knockout zebrafish

The morphological and survival features of zebrafish from 0 to 30 d.p.f. were observed and photographed using an Olympus microscope (BX51, Olympus, Japan). Abnormal

morphological phenotypes, including curved body and abdominal swelling, were observed. The survival percentage of zebrafish of each genotype was calculated using Kaplan-Meier survival analysis. For locomotion tracking, 6-9 d.p.f. larvae were placed in individual wells of a 96-well flat-bottomed culture dish (Corning, #07-200-565). Each well contained approximately 200 μL Ringer's solution and one larva. Behavior was monitored at 28.5 °C using a ZebraBox system (ViewPoint Behavior Technology) and was then analyzed using Zebralab locomotion tracking software (ViewPoint Behavior Technology). After 10 min of habituation, each larva was recorded for a total of 5 min with 5 light/dark cycles (each consisting of 10 sec on light and 50 sec off light), followed by 60 min of recording. We then calculated the traveled distance, duration, and numbers of rapid whirlpool-like circling swimming with high speed (> 20 mm/sec, characterized as seizure behavior)[12]. Videos were analyzed blindly for the classification of seizure behavior.

Electrophysiological assay on zebrafish

Electrophysiological recordings in zebrafish were obtained using the methods described in the literatures[12,13]. Briefly, 7-11 d.p.f. zebrafish larvae were embedded in a 1.2% agarose gel prepared by dissolving low-melting temperature agarose in artificial cerebrospinal fluid (aCSF) (NaCl 134 mM, KCl 2.9 mM, MgCl2 1.2 mM, CaCl2 2.1 mM, glucose 10 mM, and HEPES 10 mM) with anesthetic agent (α-bungarotoxin, 1 mg/mL, Sigma). Then, fish were placed on the upright stage of an Olympus microscope and perfused with standard recording solution. A glass microelectrode (~1 μm tip

diameter, 2-7 MΩ) was placed in the optic tectum of the fish under visual guidance. Electrodes were filled with 2 M NaCl, and electrical activity was recorded using a 700B amplifier. Traces were bandpass filtered (0.2-1 kHz). A detection threshold of three times background noise was applied to extract the events on a 5-minute-long window. Detected events were manually sorted. Two or more consecutive spikes with a threshold of three times the background noise was considered seizure-like events in a 20-minute-long window. The time and duration of each event were extracted to evaluate seizure-like electrophysiology.

***Celsr2* knockout mice/seizure and electroencephalography (EEG) recording**

Celsr2$^{-/-}$ mice were generated as previously described[14] and provided by Dr. Qu Yibo (Guangdong-Hong Kong-Macau Institute of CNS Regeneration, Jinan University). All mice were obtained by breeding *Celsr2*$^{+/-}$ males with *Celsr2*$^{+/-}$ females and maintained on a 12-hr light/dark cycle (lights on at 8:00 am, off at 8:00 pm) with food and water *ad libitum*. At three weeks old, the mice were placed into opaque home cages under 24-hr video monitoring for 7 days.

EEGs were recorded in *Celsr2*$^{-/-}$ and wild-type mice with free behavior for analysis of epileptic seizures, according to a previous study[15]. Briefly, the mice were anesthetized by 2% isoflurane (vol/vol) and implanted with a Teflon-coated silver wire electrode in the cortex (1.5 mm posterior and 1.2 mm lateral to the bregma) for signal capture. The EEG signal was synchronized with a USB video camera to analyze epileptic seizure-like behavior. EEG signals were amplified with a preamplifier and

primary amplifier (EX1, Dagan) and sampled at 10000 Hz (gain, 1000; bandpass filter, 0.1 to 500 Hz). Epileptic seizures were identified by checking both the EEG signal and the behavior of the animals. The incidence of seizures was calculated as previously described[16].

Supplementary Results

General information from WES

On average, 5.9 Gb of the sequence was produced within the exome-targeted regions in each individual, with an average coverage of 120 depths (Table S3). After variant filtration by inheritance origin and the stratified MAF (steps 2 and 3 in Fig. S1), we obtained 1112 qualified variants in 931 genes, including 177 single *de novo* (15.9%), 77 homozygous (6.9%), 725 compound heterozygous (65.2%), and 133 hemizygous variants (12%) (Table S4 and Fig. S4A). The average number of variants per case was 4.8, including 0.8 *de novo* (ranging from 0 to 4), 0.3 homozygous (ranging from 0 to 5), and 3.1 compound heterozygous variants (ranging from 0 to 10); the number of hemizygous variants per male case was 0.8 (133/163, ranging from 0 to 5) (Fig. S4B).

Genetic data of cases with *SBF1*, *CELSR2*, and *TENM1* variants

Four missense variants in *SBF1* (MIM*603560) were identified in four unrelated cases, including three *de novo* variants (c.337C>A/p.Gln113Lys, c.4459G>A/p.Gly1487Ser, and c.5424G>C/p.Trp1808Cys) and one with unknown origin (adopted, c.2272A>G/p.Ile758Val) (the DNA sequencing chromatograms in Fig. S6A). Three *de novo* missense variants (p.Gln113Lys, p.Gly1487Ser, and p.Trp1808Cys) were predicted to alter hydrogen bonding with surrounding residues (Fig. S6B), the other variant p.Ile758Val was predicted without hydrogen bond changes but was predicted to decrease the protein stability (Fig. S6B).

Biallelic variants in *CELSR2* (MIM*604265) were identified in eight unrelated cases, including a homozygous missense variant (c.7227C>A/p.His2409Gln) in two cases and six compound heterozygous missense variants (c.1763C>G/p.Pro588Arg & c.8545G>A/p.Glu2849Lys, c.3640A>T/p.Ser1214Cys & c.6108C>G/p.Phe2036Leu, c.4411C>A/p.Pro1471Thr & c.5969G>A/p.Arg1990His, c.6986G>A/p.Ser2329Asn & c.3640A>T/p.Ser1214Cys, c.8551A>G/p.Ser2851Gly & c.3329C>T/p.Thr1110Ile, and c.8624G>A/p.Arg2875Gln & c.6313A>T/p.Thr2105Ser) (the DNA sequencing chromatograms in Fig. S7A). Among the eight pairs of biallelic variants in *CELSR2*, at least one of the paired missense variants was predicted to affect hydrogen bonding or decrease protein stability (Fig. S7B).

Five hemizygous missense variants in *TENM1* (MIM*10178) were identified in six unrelated cases, including c.467A>G/p.Asp156Gly, c.503G>A/p.Cys168Tyr, c.638C>T/p.Ala213Val, c.3326C>T/p.Thr1109Met, and c.5246T>C/p.Val1756Ala (the DNA sequencing chromatograms in Fig. S8A). Among the five variants in *TENM1*, one variant (p.Cys168Tyr) was predicted to alter hydrogen bonding with surrounding residues (Fig. S8B), the other four variants were predicted without hydrogen bond changes but two of them (p.Cys168Tyr and p.Cys168Tyr) were predicted to decrease the protein stability (Fig. S8B).

Supplementary Figures

Figure S1. Flow chart of trio-based whole-exome sequencing with an individualized analytical framework

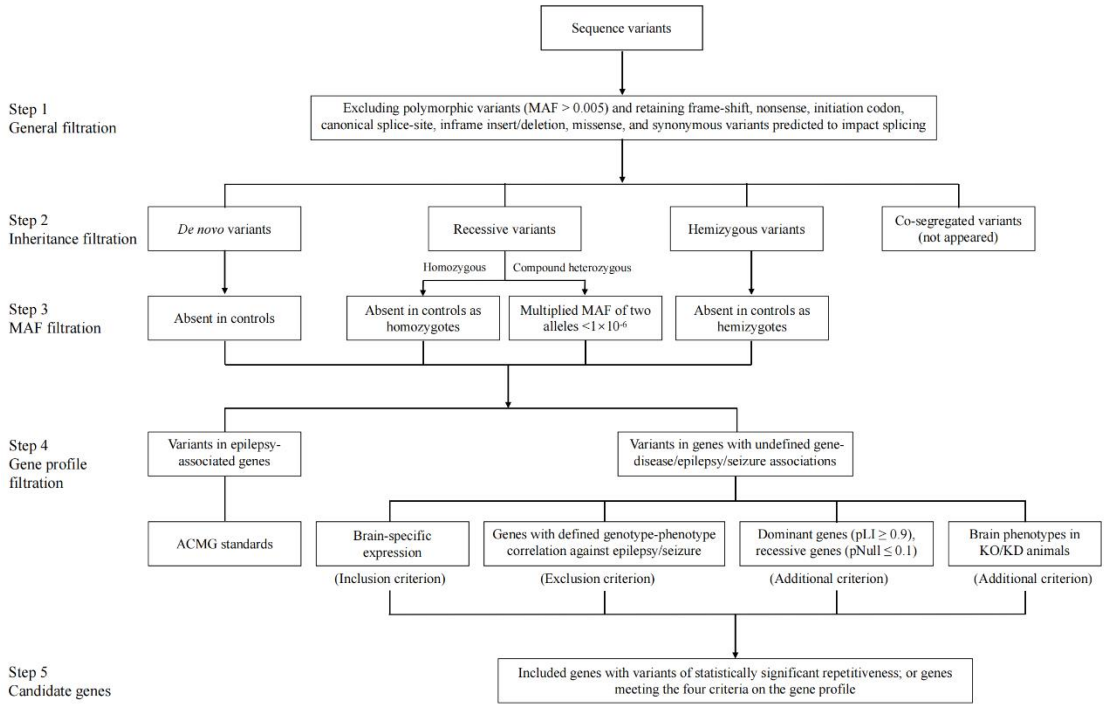

Abbreviations: ACMG, American College of Medical Genetics and Genomics guidelines; KO/KD, knockout/knockdown; MAF, minor allele frequency.

Figure S2. Knockdown efficiency of *Sbf*, *Flamingo*, and *Ten-m* in the flies

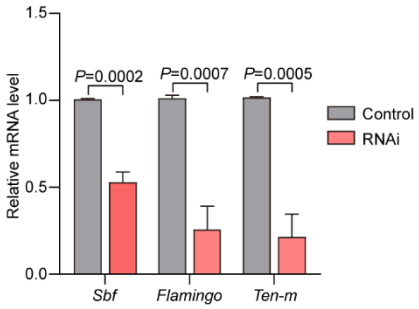

The relative mRNA levels of *Sbf*, *Flamingo*, and *Ten-m* in knockdown flies were detected by RT-qPCR. The mRNA levels of wild-type flies were normalized to 1.0. The *Gapdh* was used as an internal control. Data were analyzed by Student's t test.

Figure S3. Establishment of a *sbf1* KO zebrafish model using CRISPR/Cas9

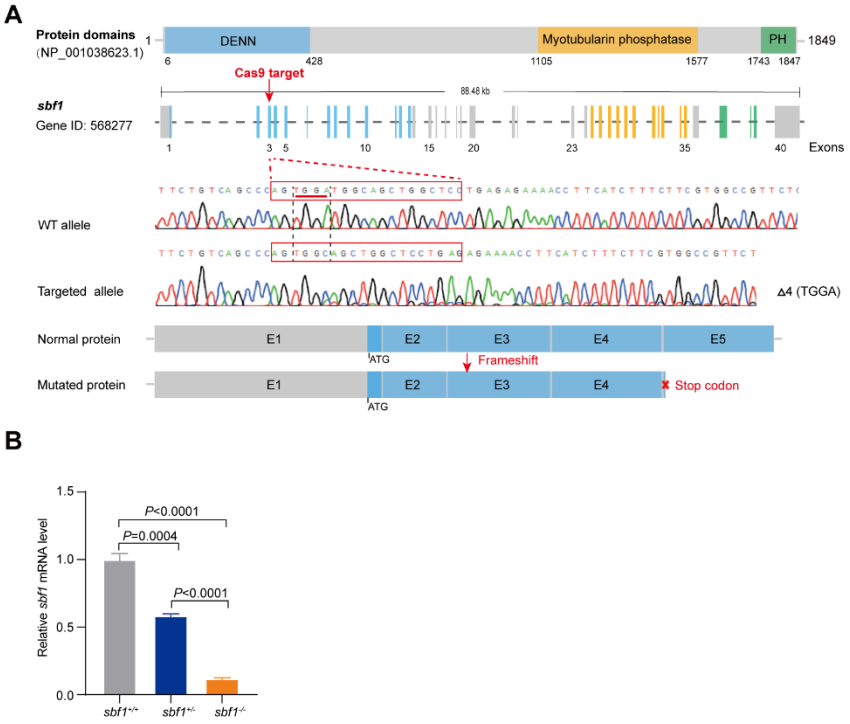

(A) The CRISPR/Cas9 gRNA targeted exon 3 (E3) of *sbf1*, resulting in a 4-nt (TGGA) deletion in E3. The frameshift mutation led to a stop codon in exon 5 (E5). **(B)** The relative mRNA expression of *sbf1* was detected by RT-qPCR in the *sbf1*$^{+/+}$, *sbf1*$^{+/-}$, and *sbf1*$^{-/-}$ fish. The mRNA levels of *sbf1*$^{+/+}$ were normalized to 1.0. The *gapdh* was used as an internal control. Data were analyzed by Student's t test.

Figure S4. General information of the variants after filtration by inheritance origin and stratified MAF

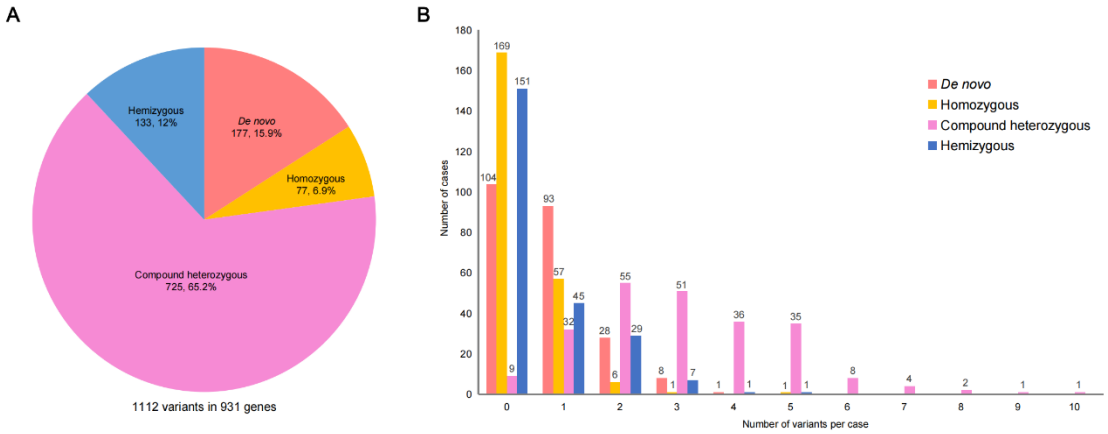

(A) Pie chart of the inheritance origin of the 1112 qualified variants. **(B)** The distribution of the number of *de novo*, homozygous, compound heterozygous, and hemizygous variants per case.

Figure S5. The frequencies of biallelic variants in LGS compared with those in the asymptomatic parent controls

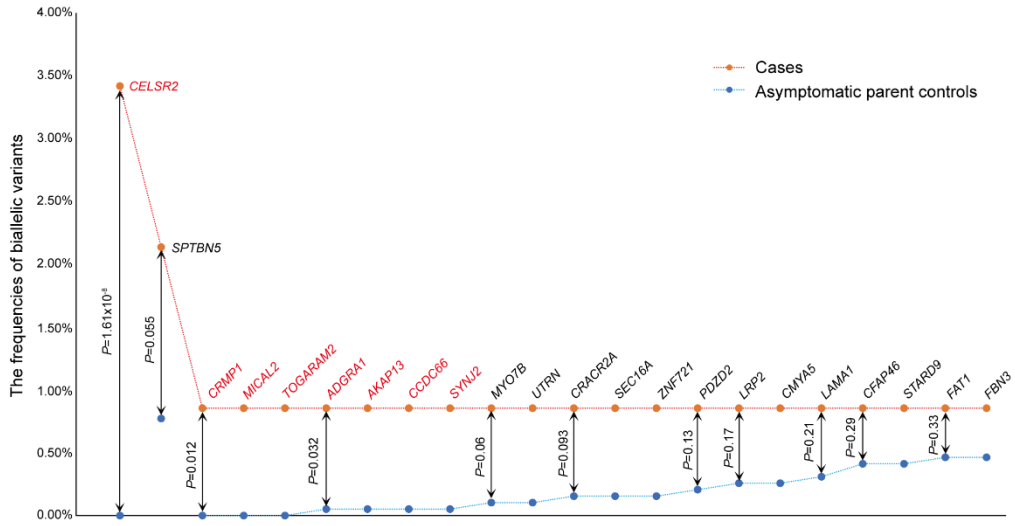

The orange dots indicate the frequencies of genes with biallelic variants in cases. The blue dots indicate the frequencies of genes with biallelic variants in asymptomatic parent controls. The genes in red font indicate that the frequencies of biallelic variants in cases were significantly higher than those in the asymptomatic parent controls. Data were analyzed by two-tailed Fisher's exact test.

Figure S6. Genetic data of cases with *SBF1* variants

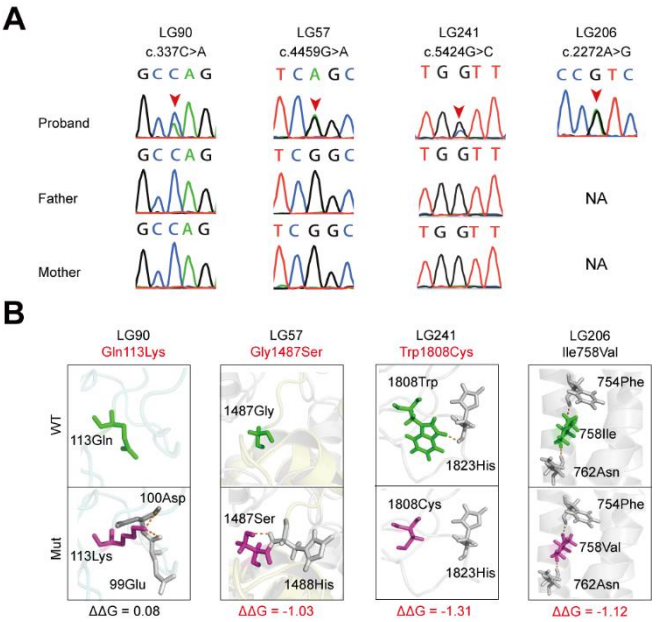

(A) Sanger sequencing verification of four cases with *SBF1* variants. **(B)** Modeling of *SBF1* missense variants indicated abnormal hydrogen bonds. Wild-type and mutant residues are colored green and light magenta, respectively. Hydrogen bonds are colored orange. The variant Lys113 rebuilds two hydrogen bonds with Asp100 and Glu99. Ser1487 rebuilds one with His1488. The variant 1808Cys destroyed one hydrogen bond with His1823. Variants that altered the stability of the global conformation of the SBF1 protein were indicated by the value of free energy stability changes (ΔΔG, Kcal/mol) using online tools (http://gpcr.biocomp.unibo.it/cgi/predictors/I-Mutant3.0/I-Mutant3.0.cgi). An absolute value of ΔΔG > 0.5 indicates a large decrease in stability. The variants in red font (the top) indicate that the variant changed hydrogen bonds with surrounding amino acid residues. The ΔΔG in red font (bottom) indicates that the variant significantly changed the protein stability.

Figure S7. Genetic data of cases with *CELSR2* variants

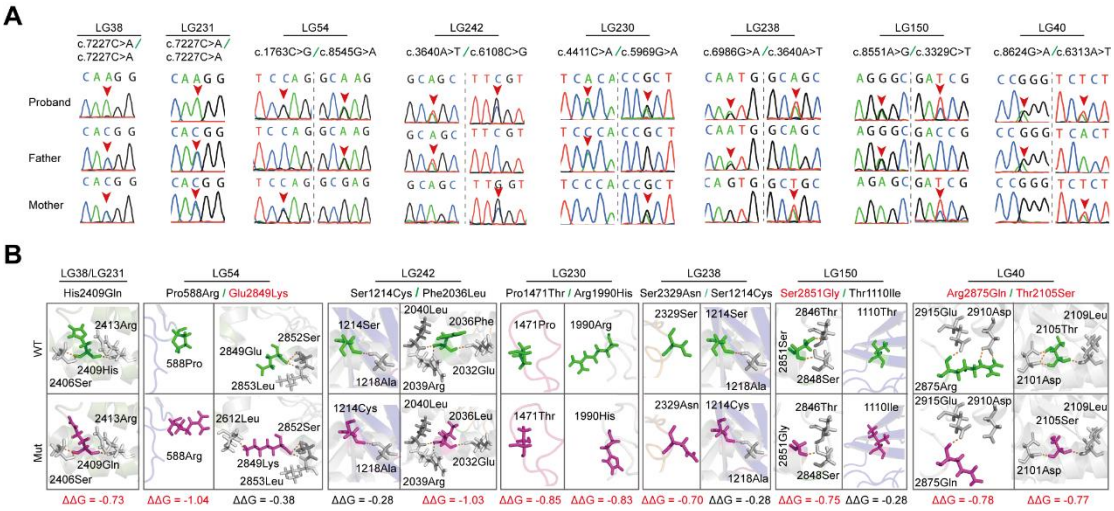

(A) Pedigrees and Sanger sequencing verification of the eight cases with biallelic *CELSR2* variants. **(B)** Modelling of CELSR2 missense variants indicated abnormal hydrogen bonds. Wild-type and mutant residues are colored green and light magenta, respectively. Hydrogen bonds are colored orange. Variants that destabilized the global conformation of the CELSR2 protein were indicated by the value of free energy stability changes (ΔΔG, Kcal/mol) using online tools (http://gpcr.biocomp.unibo.it/cgi/predictors/I-Mutant3.0/I-Mutant3.0.cgi). An absolute value of ΔΔG > 0.5 indicates a large decrease in stability. The variants in red font (the top) indicate that the variant changed hydrogen bonds with surrounding amino acid residues. The ΔΔG in red font (bottom) indicates that the variant significantly changed the protein stability.

Figure S8. Genetic data of cases with *TENM1* variants

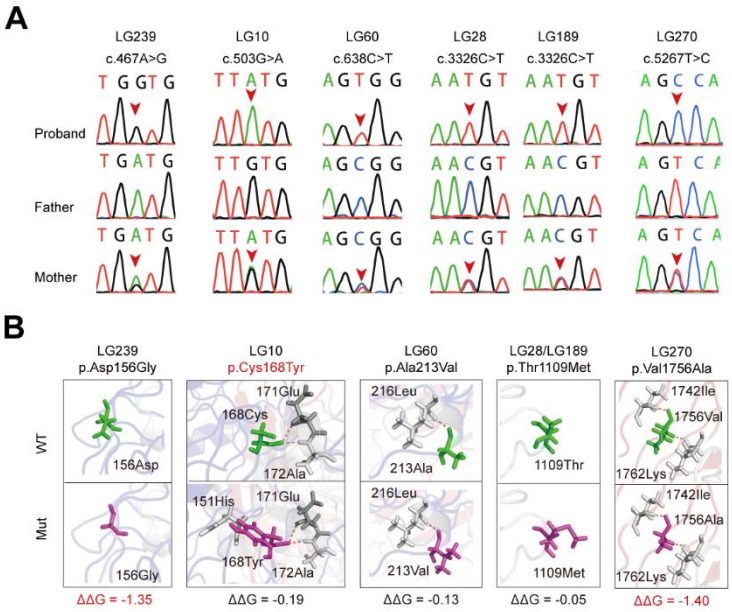

(A) Pedigrees and Sanger sequencing verification of the six cases with *TENM1* variants.

(B) Modelling of TENM1 missense variants predicted abnormal hydrogen bonds. Wild-type and mutant residues are colored green and light magenta, respectively. Hydrogen bonds are colored orange. The variant Tyr168 rebuilds a hydrogen bond with His151. Variants that destabilized the global conformation of the TENM1 protein were indicated by the value of free energy stability changes (ΔΔG, Kcal/mol) using online tools (http://gpcr.biocomp.unibo.it/cgi/predictors/I-Mutant3.0/I-Mutant3.0.cgi). An absolute value of ΔΔG > 0.5 indicates a large decrease in stability. The variants in red font (the top) indicate that the variant changed hydrogen bonds with surrounding amino acid residues. The ΔΔG in red font (bottom) indicates that the variant significantly changed the protein stability.

Figure S9. Localization of *SBF1* variants identified in this study and in Charcot-Marie-Tooth disease

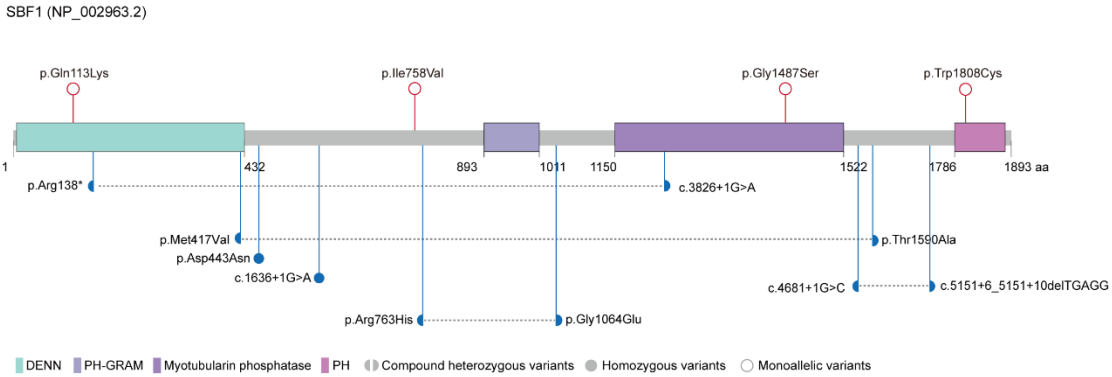

Variants identified in this study are shown in red (the top). Variants associated with Charcot-Marie-Tooth disease are shown in blue (bottom). The gray dotted lines indicate the pairs of compound heterozygous variants of *SBF1*.

Supplementary References

1. Shi, Y.W. *et al.* Synaptic clustering differences due to different GABRB3 mutations cause variable epilepsy syndromes. *Brain* **142**, 3028-3044 (2019).
2. Wang, J. *et al.* UNC13B variants associated with partial epilepsy with favourable outcome. *Brain* **144**, 3050-3060 (2021).
3. Epi, K.C. *et al. De novo* mutations in epileptic encephalopathies. *Nature* **501**, 217-21 (2013).
4. Martin, H.C. *et al*. Quantifying the contribution of recessive coding variation to developmental disorders. *Science* **362**, 1161-1164 (2018).
5. Ni, J.Q. *et al.* A genome-scale shRNA resource for transgenic RNAi in Drosophila. *Nat Methods* **8**, 405-7 (2011).
6. Parker, L., Howlett, I.C., Rusan, Z.M. & Tanouye, M.A. Seizure and epilepsy: studies of seizure disorders in Drosophila. *Int Rev Neurobiol* **99**, 1-21 (2011).
7. Perkins, K.L. Cell-attached voltage-clamp and current-clamp recording and stimulation techniques in brain slices. *J Neurosci Methods* **154**, 1-18 (2006).
8. Gu, H. & O'Dowd, D.K. Cholinergic synaptic transmission in adult Drosophila Kenyon cells in situ. *J Neurosci* **26**, 265-72 (2006).
9. Pena, I.A. *et al.* Pyridoxine-Dependent Epilepsy in Zebrafish Caused by Aldh7a1 Deficiency. *Genetics* **207**, 1501-1518 (2017).
10. Hwang, W.Y. *et al.* Efficient genome editing in zebrafish using a CRISPR-Cas system. *Nat Biotechnol* **31**, 227-9 (2013).

11. Sander, J.D. *et al.* ZiFiT (Zinc Finger Targeter): an updated zinc finger engineering tool. *Nucleic Acids Res* **38**, W462-8 (2010).
12. Baraban, S.C., Taylor, M.R., Castro, P.A. & Baier, H. Pentylenetetrazole induced changes in zebrafish behavior, neural activity and c-fos expression. *Neuroscience* **131**, 759-68 (2005).
13. Baraban, S.C. Forebrain electrophysiological recording in larval zebrafish. *J Vis Exp* https://doi.org/10.3791/50104 (2013).
14. Tissir, F. *et al.* Lack of cadherins Celsr2 and Celsr3 impairs ependymal ciliogenesis, leading to fatal hydrocephalus. *Nat Neurosci* **13**, 700-7 (2010).
15. Lin, T.W. *et al.* Regulation of Synapse Development by Vgat Deletion from ErbB4-Positive Interneurons. *J Neurosci* **38**, 2533-2550 (2018).
16. Chen, W. *et al.* Neddylation stabilizes Nav1.1 to maintain interneuron excitability and prevent seizures in murine epilepsy models. *J Clin Invest* **131**(2021).